



A Fluorescent and Colorimetric Chemosensor for Hg²⁺ Based on Rhodamine 6G With a Two-Step Reaction Mechanism

Cui-Bing Bai^{1,2}, Wei-Gang Wang¹, Jie Zhang¹, Chang Wang^{1,2}, Rui Qiao^{1,2*}, Biao Wei^{1,2}, Lin Zhang^{1,2}, Shui-Sheng Chen^{1,2} and Song Yang^{1,2}

¹ School of Chemistry and Materials Engineering, Fuyang Normal University, Fuyang, China, ² Anhui Province Key Laboratory for Degradation and Monitoring of Pollution of the Environment, Fuyang, China

A fluorescent and colorimetric chemosensor **L** based on rhodamine 6G was designed, synthesized, and characterized. Based on a two-step reaction, the chemosensor **L** effectively recognized Hg²⁺. The interaction between the chemosensor and Hg²⁺ was confirmed by ultraviolet–visible spectrophotometry, fluorescence spectroscopy, electrospray ionization–mass spectrometry, Fourier-transform infrared spectroscopy, and frontier molecular orbital calculations. The chemosensor **L** was also incorporated into test strips and silica gel plates, which demonstrated good selectivity and high sensitivity for Hg²⁺.

OPEN ACCESS

Edited by:

Yun-Bao Jiang,
Xiamen University, China

Reviewed by:

Juyoung Yoon,
Ewha Womans University,
South Korea
Tony D. James,
University of Bath, United Kingdom

*Correspondence:

Rui Qiao
qiaorui@mail.ipc.ac.cn

Specialty section:

This article was submitted to
Supramolecular Chemistry,
a section of the journal
Frontiers in Chemistry

Received: 15 May 2019

Accepted: 07 January 2020

Published: 19 February 2020

Citation:

Bai C-B, Wang W-G, Zhang J,
Wang C, Qiao R, Wei B, Zhang L,
Chen S-S and Yang S (2020) A
Fluorescent and Colorimetric
Chemosensor for Hg²⁺ Based on
Rhodamine 6G With a Two-Step
Reaction Mechanism.
Front. Chem. 8:14.
doi: 10.3389/fchem.2020.00014

Keywords: chemosensor, Hg²⁺, rhodamine 6G, test strips, silica gel plates

INTRODUCTION

Hg²⁺ is known to be very dangerous to human health because of its extreme toxicity (Chen et al., 2012). Even extremely low levels of Hg²⁺ accumulation in the human body can lead to numerous diseases in human organs (Pan et al., 2018; Peng et al., 2018; Xu et al., 2018). Thus, it is important to develop methods to detect Hg²⁺ with good sensitivity and high selectivity.

Compared to other common methods for Hg²⁺ detection, fluorescent chemosensors have received considerable attention because of their distinct advantages (Nolna and Lippard, 2008; Zhang et al., 2008; Lee et al., 2015; Xie et al., 2015; He et al., 2016; Sakunkaewkasem et al., 2018; Bai et al., 2019; Yuan et al., 2019). As a result, a growing number of fluorescent chemosensors for Hg²⁺ have been reported in the past few decades (Chen et al., 2011; Wang et al., 2012; Park et al., 2013; Cheng et al., 2015; Hong et al., 2016; Lee et al., 2016; Erdemir et al., 2017; Bai et al., 2018; Singh et al., 2018).

Many reported Hg²⁺ chemosensors were designed in one of two ways based on one-step reactions. In the first type of sensor, the interactions between a ligand and Hg²⁺ results in changes in fluorescence (**Figure 1A**). The main disadvantage of this type of sensor is its vulnerability to interference from other metal ions, especially Cu²⁺, Cd²⁺, and Fe³⁺ (Wang et al., 2011; Kau et al., 2012; Rao et al., 2012; Zhang et al., 2013; Kim et al., 2014; Fang et al., 2016; Alibert et al., 2017; Huang et al., 2019). In the second type of sensor, special chemical reactions (e.g., desulfurization between the ligands and Hg²⁺) generate a new product with a different fluorescence spectrum (**Figure 1B**).

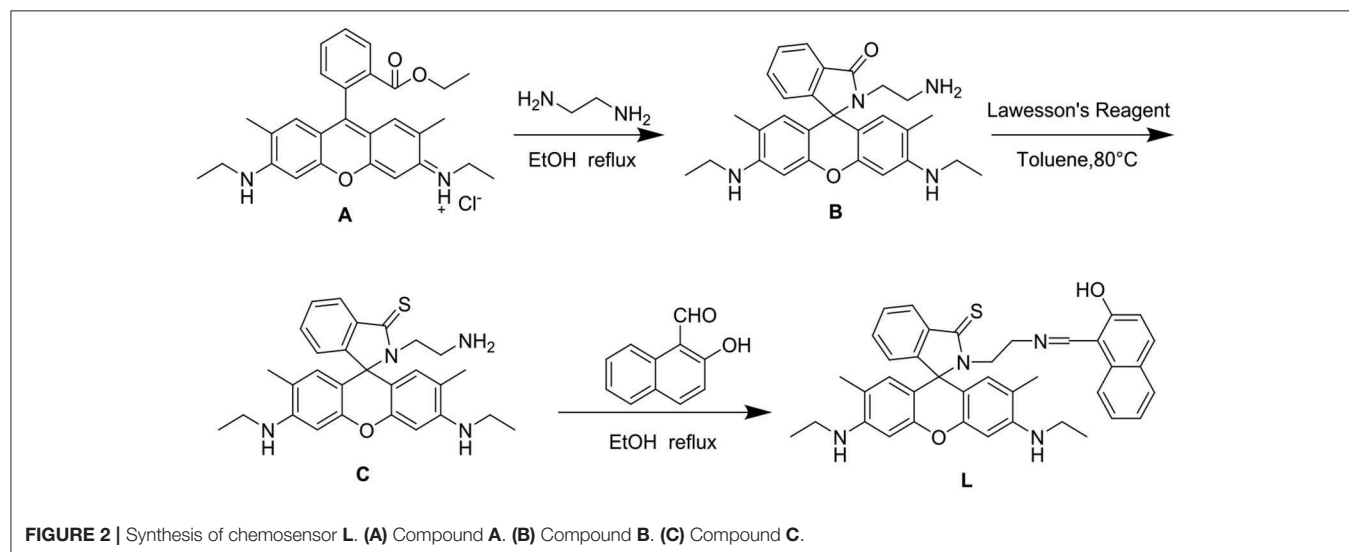
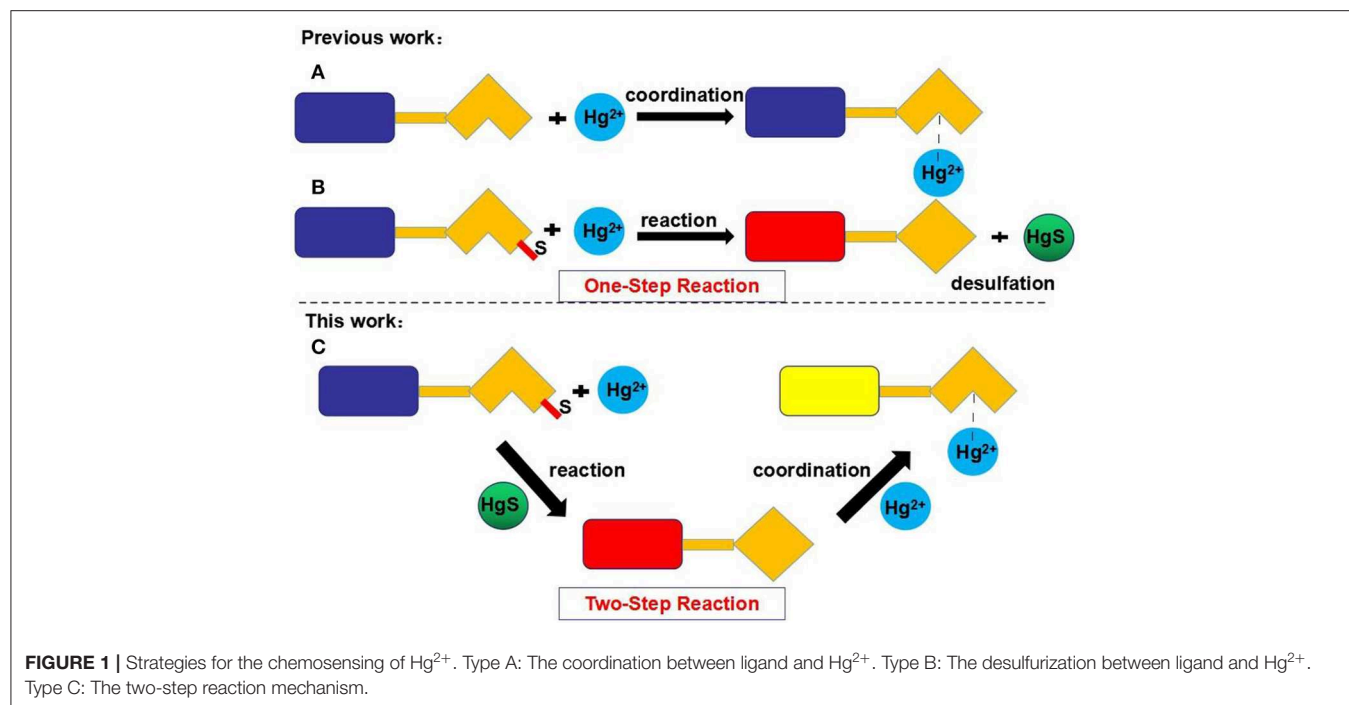
In contrast, the fluorescent chemosensor **L** developed in this study recognizes Hg²⁺ through a two-step reaction based on rhodamine 6G. The chemosensor **L** first undergoes a desulfurization

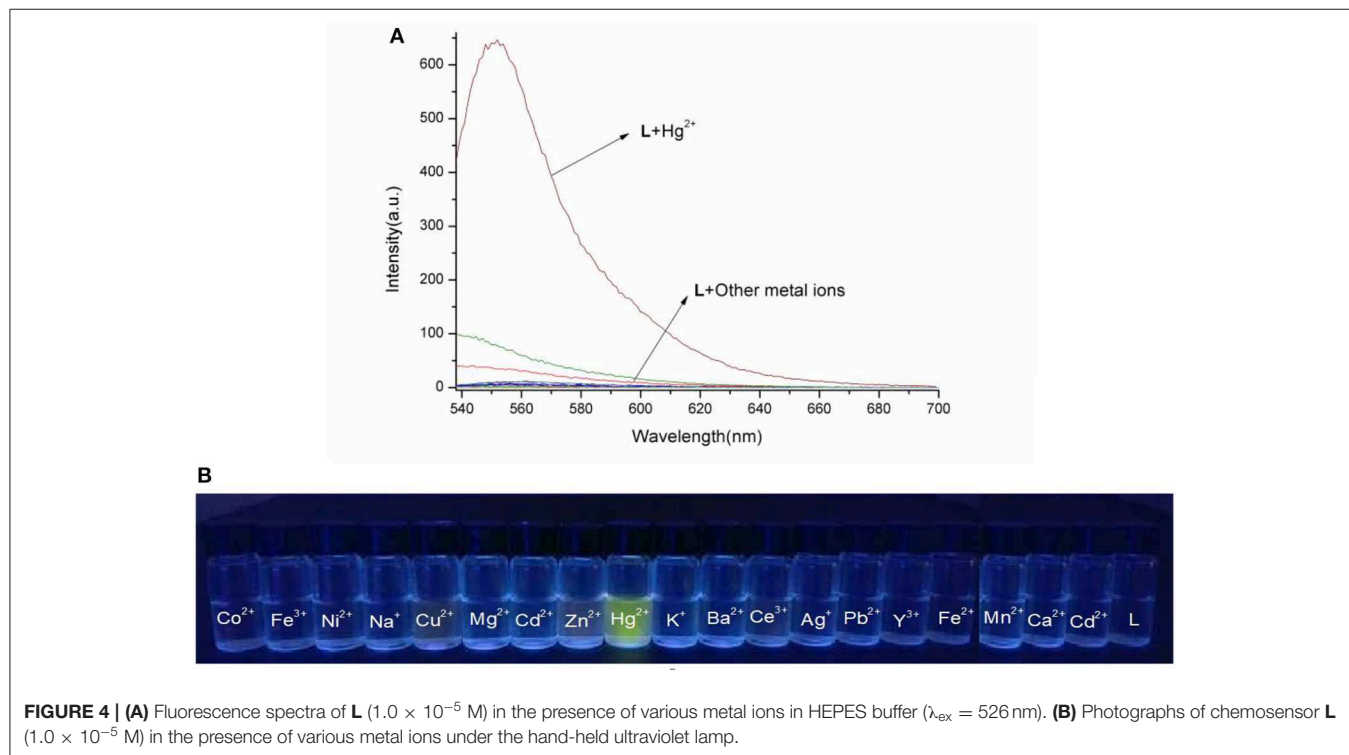
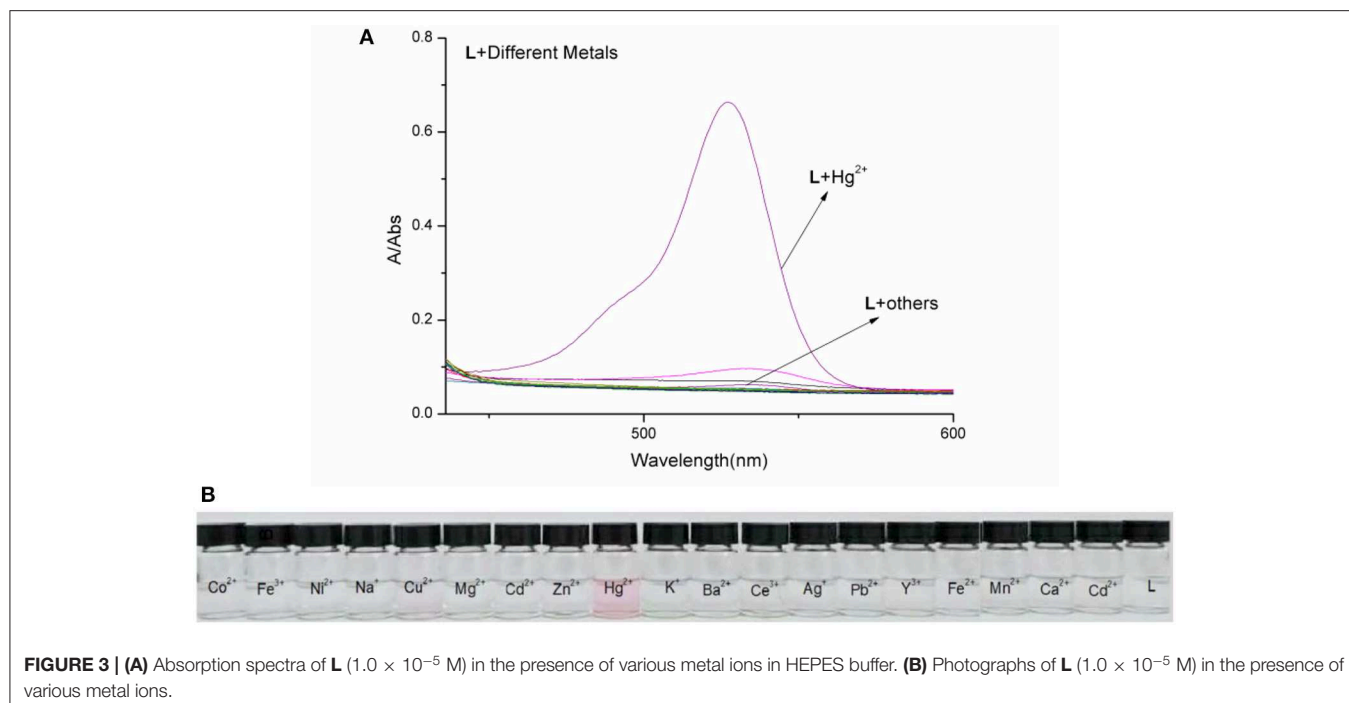
reaction with Hg²⁺, and the resulting product then interacts with Hg²⁺ (Figure 1C). As demonstrated in this study, L can selectively and sensitively detect Hg²⁺ without interference from other cations, including Cu²⁺, Cd²⁺, and Fe³⁺. Moreover, test strips and silica gel plates based on L also exhibit good selectivity for Hg²⁺.

MATERIALS AND PHYSICAL METHODS

¹H nuclear magnetic resonance (NMR) and ¹³C NMR spectra were recorded using a Bruker instrument at 400 MHz with tetramethylsilane as the internal standard and deuterated

dimethyl sulfoxide (DMSO-d₆) as the solvent. Ultraviolet-visible (UV-vis) absorption spectra were recorded on a Shimadzu UV-1601 spectrophotometer. Luminescence spectra were recorded on a Horiba Fluoromax-4-NIR spectrometer. Melting points were measured on an X-4 digital melting point apparatus (uncorrected). Infrared (IR) spectra were obtained on a Nicolet 5700 FT-IR spectrophotometer. Fluorescent lifetime and fluorescence quantum yield were measured using a Horiba Fluoromax-4 spectrometer. For fluorescent lifetime measurements, the fluorescence signals were collimated and focused onto the entrance slit of a monochromator, and the output plane was equipped with a photomultiplier tube. The fluorescent decay was then analyzed by least-squares regression,





and the quality of the exponential fit was evaluated by the goodness of fit (χ^2). Mass spectra were recorded with a Shimadzu LCMS-IT/TOF mass spectrometer. All reagents used were of analytical grade.

Synthesis of Compound L

The synthesis of **L** is outlined in **Figure 2**. Compound **C** was synthesized according to the reported procedure (Hong et al., 2016). Compound **C** (0.5 mmol) and

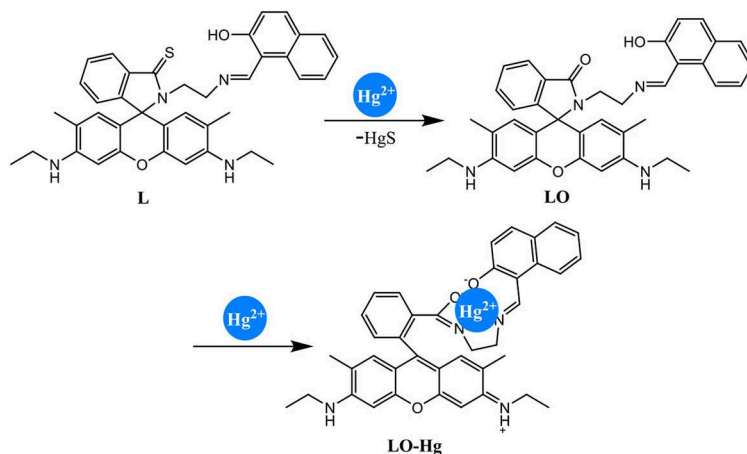


FIGURE 5 | Proposed mechanism for Hg²⁺ detection by chemosensor **L**.

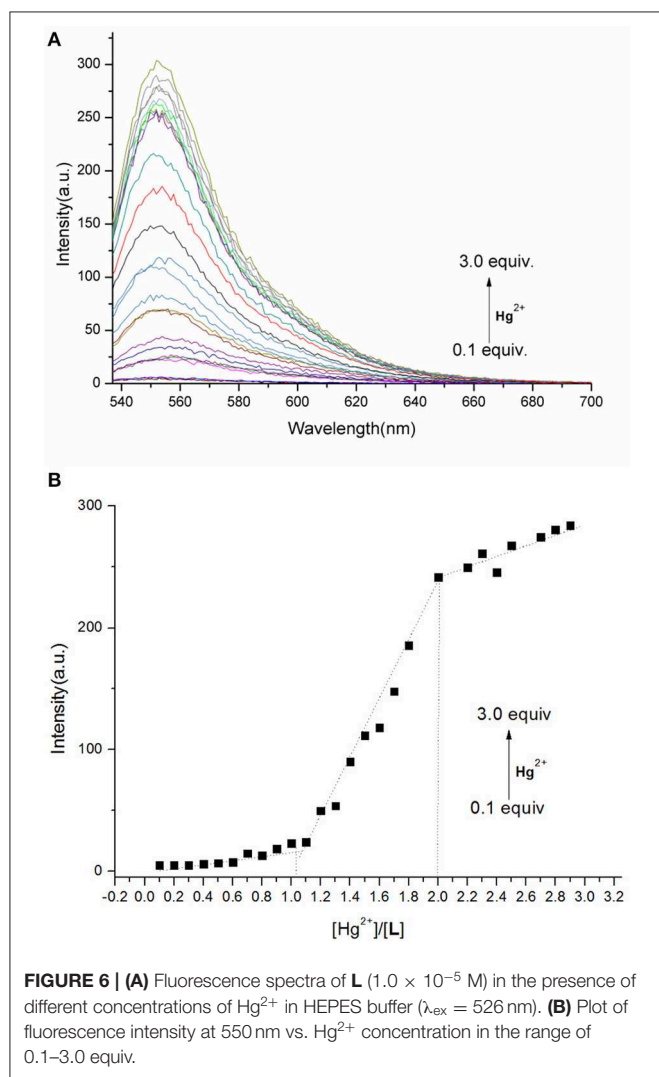


FIGURE 6 | **(A)** Fluorescence spectra of **L** (1.0×10^{-5} M) in the presence of different concentrations of Hg²⁺ in HEPES buffer ($\lambda_{\text{ex}} = 526$ nm). **(B)** Plot of fluorescence intensity at 550 nm vs. Hg²⁺ concentration in the range of 0.1–3.0 equiv.

2-hydroxy-1-naphthaldehyde (0.5 mmol) were then dissolved in 20 ml of ethanol and refluxed for 12 h with stirring, forming an orange precipitate. The crude product was filtered and purified by silica gel chromatography (ethyl acetate:petroleum ether = 3:1) to obtain the fluorescent chemosensor **L**. Yield 81%, m.p. >300°C, ¹H NMR (see **Figure S1**) (400 MHz, DMSO-d₆, δ): 13.84 (s, 1H), 8.76 (d, $J = 8.7$ Hz, 1H), 7.98 (dd, $J = 5.4, 3.2$ Hz, 1H), 7.92 (d, $J = 8.4$ Hz, 1H), 7.72 (d, $J = 9.3$ Hz, 1H), 7.64 (d, $J = 7.5$ Hz, 1H), 7.59 (dd, $J = 6.0, 2.6$ Hz, 2H), 7.42 (t, $J = 7.2$ Hz, 1H), 7.21 (t, $J = 7.3$ Hz, 1H), 7.07 (dd, $J = 5.3, 3.0$ Hz, 1H), 6.72 (d, $J = 9.3$ Hz, 1H), 6.32 (s, 2H), 6.01 (s, 2H), 5.12 (s, 2H), 3.76 (t, $J = 6.7$ Hz, 2H), 3.12 (dd, $J = 9.2, 5.8$ Hz, 4H), 1.81 (s, 6H), 1.20 (t, $J = 7.1$ Hz, 6H). ¹³C NMR (see **Figure S2**) (100 MHz, DMSO) δ 191.24, 175.39, 159.96, 151.58, 151.49, 148.69, 137.52, 137.11, 134.29, 133.46, 129.31, 129.25, 128.26, 127.65, 125.93, 125.03, 124.94, 123.77, 122.80, 119.19, 119.00, 106.77, 103.12, 96.17, 73.51, 49.53, 44.63, 37.92, 17.53, 14.56. HRMS (ESI, see **Figure S3**) m/z : [M+H]⁺ Calcd for C₃₉H₃₉N₄O₂S: 627.2788; Found 627.2786.

General Spectroscopic Methods

A solution of metal ions was prepared from the nitrate salts of K⁺, Na⁺, Ag⁺, Cu²⁺, Co²⁺, Ca²⁺, Cd²⁺, Mg²⁺, Ba²⁺, Pb²⁺, Fe²⁺, Ni²⁺, Zn²⁺, Mn²⁺, Hg²⁺, Al³⁺, Y³⁺, Ce³⁺, and Fe³⁺ (China Pharmaceutical Co. Ltd., used without further purification). The ligand concentration was kept constant at 1.0×10^{-5} M during spectral measurements. The probe solution was prepared in HEPES buffer (10 mM, pH 7.4)/CH₃CN (40:60, V/V).

RESULTS AND DISCUSSION

The spectral properties of **L** were studied in HEPES buffer (**Figures 3, 4**). When the concentration of Hg²⁺ increased to 10 equivalents, a new absorption peak at 526 nm appeared (**Figure 3**). In the fluorescence spectrum, an emission peak appeared at 550 nm upon excitation at 526 nm (**Figure 4**). The

other cations did not result in the same spectral changes as Hg²⁺. Meanwhile, the color of the solution also changed significantly when 10 equivalents of Hg²⁺ was added to **L**. This color change could be observed directly by the naked eye.

Based on competition experiments, the detection of Hg²⁺ by **L** was not affected by the presence of other cations, including Cu²⁺, Cd²⁺, and Fe³⁺ (Figures S4, S5, ESI). Surprisingly, the spectral properties depended on the ratio of [Hg²⁺] to [**L**]. When the ratio did not exceed 1, the spectra did not change markedly before or after Hg²⁺ was added into the solution of **L**. The emission peak at 550 nm did not appear (Figures S6, S7, ESI), while no change was observed in the UV–vis spectrum. The fluorescence intensity at 550 nm increased strongly when the ratio exceeded 1, and a new absorption peak at 526 nm appeared. These results are unusual in comparison to previously reported chemosensors for Hg²⁺ (Figures 3, 4).

To clarify the unusual results, electrospray ionization–mass spectrometry (ESI-MS) was conducted with different ratios of [Hg²⁺] to [**L**]. When the ratio did not exceed 1, the ion peak was detected at 611.3018 (*m/z*), corresponding to the desulfurization reaction product **LO** (Figure S8, ESI). This implies that **L** was transformed to **LO** under the action of Hg²⁺ provided that the ratio of [Hg²⁺] to [**L**] did not exceed 1 (Figure 5). Under this condition, Hg²⁺ did not lead to the spiro lactam ring opening of **L**. Thus, the fluorescent emission peak at 550 nm did not appear, nor did the absorption peak at 526 nm. Meanwhile, no color change of the solution was observed by the naked eye. The first desulfurization step was completed when [Hg²⁺]:[**L**] = 1. When the ratio exceeded 1, the ion peak at *m/z* 813.2609 was classified as [**LO**-Hg²⁺+H⁺]⁺ (Figure S9, ESI). Under these conditions, Hg²⁺ caused spiro lactam ring opening, generating the emission peak at 550 nm and the absorption peak at 526 nm. In addition, the solution color changed from colorless to pink. After the completion of the first step, Hg²⁺ transformed the closed spiro lactam structure into a ring-opened amide in the second step.

The IR spectra support the above two-step reaction mechanism (Figure S10, ESI). The peak at 1,153 cm⁻¹, which was assigned to the stretching vibration of C=S, disappeared during the first step. The peak at 1,518 cm⁻¹, corresponding to the stretching vibration of C=O, vanished in the second step. Therefore, **L** detected Hg²⁺ through a two-step reaction (Figure 5).

To understand the interaction between the chemosensor **L** and Hg²⁺, a titration experiment was carried out. The fluorescent

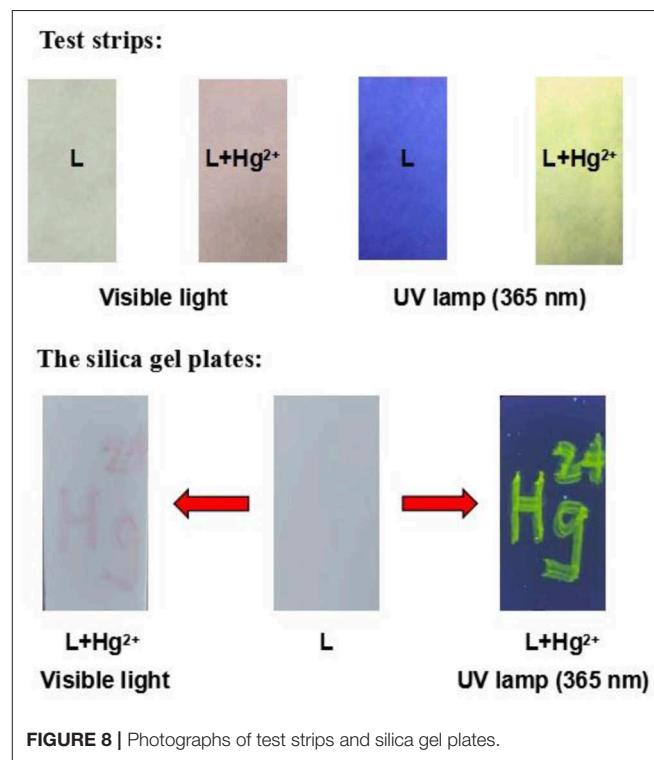


FIGURE 8 | Photographs of test strips and silica gel plates.

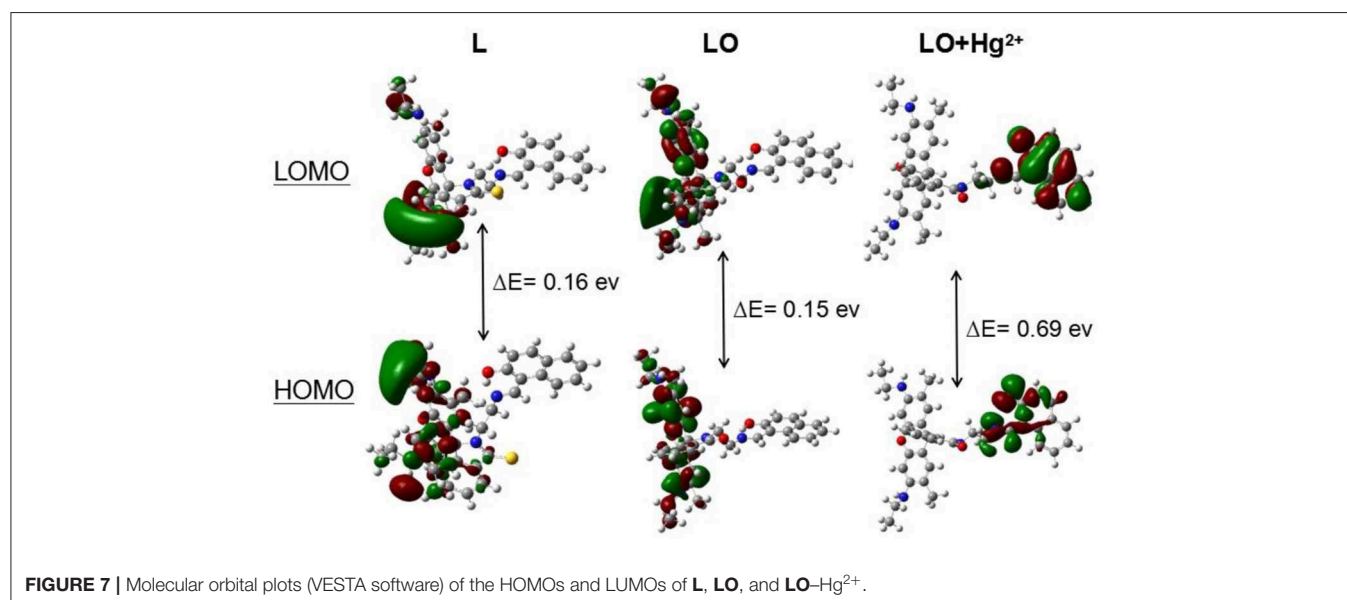


FIGURE 7 | Molecular orbital plots (VESTA software) of the HOMOs and LUMOs of **L**, **LO**, and **LO**-Hg²⁺.

intensity at 550 nm hardly changed when [Hg²⁺]:[L] changed from 0 to 1, and the absorption spectrum of **L** did not change significantly. However, the fluorescent intensity increased sharply when [Hg²⁺]:[L] changed from 1 to 2, and the intensity of the new absorption peak at 526 nm increased greatly. As shown in **Figure 3**, two inflection points were observed in the absorption spectrum of **L** + Hg²⁺, indicating that **L** might interact with Hg²⁺ in two steps. The stoichiometric ratio between **L** and Hg²⁺ was 1:1 or 1:2. The above results are in accordance with the Job plot (**Figure 6** and **Figures S11–S13**, ESI).

The calculated frontier molecular orbitals and energy levels of **L**, **LO**, and **LO–Hg²⁺** confirmed the interaction between **L** and Hg²⁺. As shown in **Figure 7**, the molecular orbital structure of **L** was clearly different from those of **LO** and **LO–Hg²⁺**. The energy gaps between the highest occupied molecular orbital (HOMO) and lowest unoccupied molecular orbital (LUMO) in **L**, **LO**, and **LO–Hg²⁺** were calculated to be 0.16, 0.15, and 0.69 eV, respectively. The results indicate that Hg²⁺ and **L** were combined via a two-step reaction, which effectively decreased the energy gap and stabilized the system.

The detection limit of **L** toward Hg²⁺ was determined to be 0.012×10^{-7} M (**Figure S14**, ESI). Moreover, the fluorescence lifetime and fluorescence quantum yield of **L–Hg²⁺** were measured to study the fluorescent properties of **L** (**Table S1**, ESI).

To evaluate the practical application potential of the chemosensor **L**, test strips and silica gel plates were prepared using **L**. When Hg²⁺ was added to the test strips, a clear change in color from colorless to pink was observed, and the fluorescence was enhanced (**Figure 8**). In addition, when “Hg²⁺” was written on the silica gel plate using Hg²⁺ solution, the silica gel plate underwent significant changes. The results indicate that **L** can be used to create smart materials for the detection of Hg²⁺ in aqueous solution.

CONCLUSIONS

In summary, a chemosensor **L** based on rhodamine 6G was designed, synthesized, and characterized. **L** was demonstrated to sensitively and selectively recognize Hg²⁺ via a two-step reaction, different from the one-step mechanisms by which reported chemosensors interact with Hg²⁺. The interaction between **L** and

Hg²⁺ was confirmed by UV–vis spectrophotometry, fluorescence spectroscopy, ESI-MS, IR spectroscopy, and frontier molecular orbital calculations. In addition, **L** could be incorporated into test strips and silica gel plates to effectively detect Hg²⁺.

DATA AVAILABILITY STATEMENT

All datasets generated for this study are included in the article/**Supplementary Material**.

AUTHOR CONTRIBUTIONS

C-BB and RQ designed the work and wrote the manuscript. C-BB, W-GW, JZ, BW, and LZ carried out the experiments. CW, S-SC, and SY performed the spectroscopic experiments. RQ revised and edited the manuscript. All authors reviewed the manuscript and have agreed to its publication.

FUNDING

This work was supported by the National Natural Science Foundation of China (No. 21302019), Anhui Provincial Natural Science Foundation (No. 1908085QB78), the Key Projects of Natural Science Research of Anhui Province Colleges and Universities (No. KJ2019ZD38), the Key Projects of Support Program for Outstanding Young Talents in Anhui Province Colleges and Universities (No. gxyqZD2016068), the Key Program for Young Talents of Fuyang Normal University (No. rcxm201902), National Undergraduate Training Programs for Innovation and Entrepreneurship (Nos. 201810371058 and 201810371054), and the Horizontal Cooperation Project of Fuyang Municipal Government and Fuyang Normal University (Nos. XDHX201730 and XDHX201731).

SUPPLEMENTARY MATERIAL

The Supplementary Material for this article can be found online at: <https://www.frontiersin.org/articles/10.3389/fchem.2020.00014/full#supplementary-material>

REFERENCES

- Alibert, A., Vaiano, P., Caporale, A., Consales, M., Ruvo, M., and Cusano, A. (2017). Fluorescent chemosensors for Hg²⁺ detection in aqueous environment. *Sens. Actuators B Chem.* 247, 727–735. doi: 10.1016/j.snb.2017.03.026
- Bai, C. B., Fan, H. Y., Qiao, R., Wang, S. N., Wei, B., Meng, Q., et al. (2019). Synthesis of methionine methyl ester-modified coumarin as the fluorescent-colorimetric chemosensor for selective detection Cu²⁺ with application in molecular logic gate. *Spectrochim. Acta. A* 216, 45–51. doi: 10.1016/j.saa.2019.03.016
- Bai, C. B., Qiao, R., Liao, J. X., Xiong, W. Z., Zhang, J., Chen, S. S., et al. (2018). A highly selective and reversible fluorescence “off-on-off” chemosensor for Hg²⁺ based on rhodamine-6G dyes derivative and its application as a molecular logic gate. *Spectrochim. Acta. A* 202, 252–259. doi: 10.1016/j.saa.2018.05.050
- Chen, X., Pradhan, T., Wang, F., Kim, J. S., and Yoon, J. (2011). Fluorescent chemosensors based on spiroring-opening of xanthenes and related derivatives. *Chem. Rev.* 112, 1910–1956. doi: 10.1021/cr200201z
- Chen, Y., Zhu, C., Yang, Z., Li, J., Jiao, Y., He, W., et al. (2012). A new “turn-on” chemodosimeter for Hg²⁺: ICT fluorophore formation via Hg²⁺-induced carbaldehyde recovery from 1, 3-dithiane. *Chem. Commun.* 48, 5094–5096. doi: 10.1039/c2cc31217d
- Cheng, H. Z., Li, G., and Liu, M. (2015). A metal-enhanced fluorescence sensing platform based on new mercapto rhodamine derivatives for reversible Hg²⁺ detection. *J. Hazard. Mater.* 287, 402–411. doi: 10.1016/j.jhazmat.2015.01.046
- Erdemir, S., Yuksekogul, M., Karakurt, S., and Kocyigit, O. (2017). Dual-channel fluorescent probe based on bisphenol a-rhodamine for Zn²⁺ and Hg²⁺ through different signaling mechanisms and its bioimaging studies. *Sens. Actuators B Chem.* 241, 230–238. doi: 10.1016/j.snb.2016.10.082

- Fang, Y. W., Zhang, B. G., Chen, J., Kong, L., Yang, L. M., Bi, H., et al. (2016). An active probe for specific sensing of Hg²⁺ based on linear conjugated bis-schiff base. *Sens. Actuators B Chem.* 229, 338–346. doi: 10.1016/j.snb.2016.01.130
- He, W. L., Dong, L. B., Liu, Y., and Lin, Y. W. (2016). Fluorescent chemosensors manipulated by dual/triple interplaying sensing mechanisms. *Chem. Soc. Rev.* 45, 6449–6461. doi: 10.1039/C6CS00413J
- Hong, M., Lu, X., Chen, Y., and Xu, D. (2016). A novel rhodamine-based colorimetric and fluorescent sensor for Hg²⁺ in water matrix and living cell. *Sens. Actuators B Chem.* 232, 28–36. doi: 10.1016/j.snb.2016.03.125
- Huang, L., Yang, Z., Zhou, Z., Li, Y., Tang, S., Xiao, W., et al. (2019). A dual colorimetric and near-infrared fluorescent turn-on probe for Hg²⁺ detection and its applications. *Dyes Pigments* 163, 118–125. doi: 10.1016/j.dyepig.2018.11.047
- Kau, P., Kau, S., and Singh, K. (2012). Bis (N-methylindolyl). methane-based chemical probes for Hg²⁺ and Cu²⁺ and molecular implication gate operating in fluorescence mode. *Org. Biomol. Chem.* 10, 1497–1501. doi: 10.1039/c2ob06793e
- Kim, I., Lee, E. N., Jeong, J. Y., Chung, H. Y., Cho, K. B., and Lee, E. (2014). Micellar and vesicular nanoassemblies of triazole-based amphiphilic probes triggered by mercury, (II) ions in a 100% aqueous medium. *Chem. Commun.* 50, 14006–14009. doi: 10.1039/C4CC06742H
- Lee, J. J., Kim, S. Y., Nam, E., Lee, Y. S., Lim, H. M., and Kim, C. (2016). A PET-based fluorometric chemosensor for the determination of mercury (II) and pH, and hydrolysis reaction-based colorimetric detection of hydrogen sulfide. *Dalton Trans.* 45, 5700–5712. doi: 10.1039/C6DT0147E
- Lee, M., Kim, S. J., and Sessler, L. J. (2015). Small molecule-based ratiometric fluorescence probes for cations, anions, and biomolecules. *Chem. Soc. Rev.* 44, 4185–4191. doi: 10.1039/C4CS00280F
- Nolna, M. E., and Lippard, J. S. (2008). Tools and tactics for the optical detection of mercuric ion. *Chem. Rev.* 108, 3443–3480. doi: 10.1021/cr068000q
- Pan, L. S., Li, K., Li, L. L., Li, Y. M., Shi, L., and Liu, H. Y. (2018). A reaction-based ratiometric fluorescent sensor for the detection of Hg(II) ions in both cells and bacteria. *Chem. Commun.* 54, 4955–4958. doi: 10.1039/C8CC01031E
- Park, S., Kim, W., Swamy, K. M. K., Lee, H. Y., Jung, J. Y., Kim, G., et al. (2013). Rhodamine hydrazone derivatives bearing thiophene group as fluorescent chemosensors for Hg²⁺. *Dyes Pigments* 99, 323–328. doi: 10.1016/j.dyepig.2013.05.015
- Peng, D., Zhang, L., Liang, P. R., and Qiu, D. J. (2018). Rapid detection of mercury ions based on nitrogen-doped graphene quantum dots accelerating formation of manganese porphyrin. *ACS Sens.* 3, 1040–1047. doi: 10.1021/acssensors.8b00203
- Rao, S. A., Kim, D. Y., Wang, J. T., Kim, H. K., Wang, H. S., and Ahn, H. K. (2012). Reaction-based two-photon probes for mercury ions: fluorescence imaging with dual optical windows. *Org. Lett.* 14, 2598–2601. doi: 10.1021/ol3009057
- Sakunkaewkasem, S., Petdum, A., Panchan, W., Sirirak, J., Charoenpanich, A., Sooksimuang, T., et al. (2018). Dual-analyte fluorescent sensor based on [5] helicene derivative with super large Stokes shift for the selective determinations of Cu²⁺ or Zn²⁺ in buffer solutions and its application in a living cell. *ACS Sens.* 3, 1016–1023. doi: 10.1021/acssensors.8b00158
- Singh, G., Ran, S., Sharma, G., Kalra, P., Singh, N., and Verma, V. (2018). Coumarin-derived organosilatrane: functionalization at magnetic silica surface and selective recognition of Hg²⁺ ion. *Sens. Actuators B Chem.* 266, 861–872. doi: 10.1016/j.snb.2018.03.036
- Wang, F., Nam, S. W., Guo, Z., Park, S., and Yoon, J. (2012). A new rhodamine derivative bearing benzothiazole and thiocarbonyl moieties as a highly selective fluorescent and colorimetric chemodosimeter for Hg²⁺. *Sens. Actuators B Chem.* 161, 948–953. doi: 10.1016/j.snb.2011.11.070
- Wang, Y., Huang, Y., Li, B., Zhang, L., Song, H., Jiang, H., et al. (2011). A cell compatible fluorescent chemosensor for Hg²⁺ based on a novel rhodamine derivative that works as a molecular keypad lock. *RSC Adv.* 1, 1294–1300. doi: 10.1039/c1ra00488c
- Xie, H. P., Guo, Q. F., Wang, Y. L., Yang, S., Yao, H. D., and Yang, Y. G. (2015). A dansyl-rhodamine ratiometric fluorescent probe for Hg²⁺ based on fret mechanism. *J. Fluoresc.* 25, 319–325. doi: 10.1007/s10895-015-1511-7
- Xu, D., Yu, S., Yin, Y., Wang, S., Lin, Q., and Yuan, Z. (2018). Sensitive colorimetric Hg²⁺ detection via amalgamation-mediated shape transition of gold nanostars. *Front. Chem.* 6:566. doi: 10.3389/fchem.2018.00566
- Yuan, X., Leng, H. T., Guo, Q. Z., Wang, Y. C., Li, Z. J., Yang, W. W., et al. (2019). A fret-based dual-channel turn-on fluorescence probe for the detection of Hg²⁺ in living cells. *Dyes Pigments* 161, 403–410. doi: 10.1016/j.dyepig.2018.09.078
- Zhang, P., Shi, B. B., Zhang, Y. M., Lin, Q., Yao, H., and You, X. M., et al. (2013). A selective fluorogenic chemodosimeter for Hg²⁺ based on the dimerization of desulfurized product. *Tetrahedron* 69, 10292–10298. doi: 10.1016/j.tet.2013.10.024
- Zhang, X., Xiao, Y., and Qian, X. (2008). A ratiometric fluorescent probe based on fret for imaging Hg²⁺ ions in living cells. *Angew. Chem. Int. Ed.* 47, 8025–8029. doi: 10.1002/anie.200803246

Conflict of Interest: The authors declare that the research was conducted in the absence of any commercial or financial relationships that could be construed as a potential conflict of interest.

Copyright © 2020 Bai, Wang, Zhang, Wang, Qiao, Wei, Zhang, Chen and Yang. This is an open-access article distributed under the terms of the Creative Commons Attribution License (CC BY). The use, distribution or reproduction in other forums is permitted, provided the original author(s) and the copyright owner(s) are credited and that the original publication in this journal is cited, in accordance with accepted academic practice. No use, distribution or reproduction is permitted which does not comply with these terms.